

ACCELERATED COMMUNICATION

Cloning and Functional Expression of a Human Liver Organic Cation Transporter

LEI ZHANG, MARK J. DRESSER, ANDREW T. GRAY, SPENCER C. YOST, SHIGEYUKI TERASHITA, and KATHLEEN M. GIACOMINI

Departments of Biopharmaceutical Sciences (L.Z., M.J.D., S.T., K.M.G.) and Anesthesia (A.T.G., S.C.Y.), University of California San Francisco, San Francisco, California 94143

Received February 7, 1997; Accepted March 6, 1997

SUMMARY

Polyspecific organic cation transporters in the liver mediate the elimination of a wide array of endogenous amines and xenobiotics. In contrast to our understanding of the mechanisms of organic cation transport in rat liver, little is known about the mechanisms of organic cation transport in the human liver. We report the cloning, sequencing, and functional characterization of the first human polyspecific organic cation transporter from liver (hOCT1). hOCT1 (554 amino acids) is 78% identical to the previously cloned organic cation transporter from rat, rOCT1 [*Nature (Lond.)* 372:549–552 (1994)]. In *Xenopus laevis* oocytes injected with the cRNA of hOCT1, the specific uptake of the organic cation ³H-1-methyl-4-phenylpyridinium (³H-MPP⁺) was significantly enhanced (8-fold) over that in water-injected oocytes. Uptake of ³H-MPP⁺ was saturable ($K_m = 14.6 \pm 4.39 \mu\text{M}$) and sensitive to membrane potential. Both small monova-

lent organic cations such as tetraethylammonium and *N*¹-methyl-4-phenylpyridinium and bulkier organic cations (e.g., vecuronium and decynium-22) inhibited the uptake of ³H-MPP⁺. In addition, the bile acid taurocholate inhibited the uptake of ³H-MPP⁺ in oocytes expressing hOCT1. Northern analysis demonstrated that the mRNA transcript of hOCT1 is expressed primarily in the human liver, whereas the mRNA transcript of rOCT1 is found in rat kidney, liver, intestine, and colon [*Nature (Lond.)* 372:549–552 (1994)]. In comparison to rOCT1, hOCT1 exhibits notable differences in its kinetic characteristics and tissue distribution. The functional expression of hOCT1 will provide a powerful tool for elucidation of the mechanisms of organic cation transport in the human liver and understanding of the mechanisms involved in the disposition and hepatotoxicity of drugs.

Polyspecific organic cation transporters in the liver are critical in the systemic and presystemic elimination of many endogenous amines as well as a wide array of drugs and environmental toxins (1–7). To mediate elimination (or excretion), transporters on the sinusoidal membrane of the hepatocyte function in the uptake of organic cations from the blood into the intracellular space. Once in the hepatocyte, organic cations may be sequestered, metabolized, or transported across the canalicular membrane into the biliary tract.

At least five organic cation transporters on the sinusoidal membrane of the rat hepatocyte have been described (5). Of

these, two organic cation-selective transporters seem to mediate the uptake of exogenous organic cations (type I and type II). The type I carrier accepts small monovalent organic cations such as tributylmethylammonium, TEA, and MPP⁺, whereas the type II carrier accepts larger organic cations that are mostly bivalent. In addition, a multispecific, non-charge-selective transporter seems to mediate the uptake of a number of compounds, including various organic cations, across the sinusoidal membrane (7).

Recently, a polyspecific transporter for organic cations (rOCT1) was cloned from a rat kidney cDNA library (8). Northern analysis revealed that rOCT1 was also found in rat liver. Subsequent studies suggest that in the liver, rOCT1 represents a transporter for organic cations on the sinusoidal membrane, which mediates the uptake of both type I and type II substances (9).

This study was supported by grants from the National Institutes of Health (GM36780 and GM26691). M.D. was supported in part by a grant from the ARCS Foundation, and S.T. was supported by Fujisawa Pharmaceutical Company.

ABBREVIATIONS: TEA, tetraethylammonium; MPP⁺, 1-methyl-4-phenylpyridinium; hOCT1, human organic cation transporter; rOCT1, rat organic cation transporter; PAH, *para*-aminohippurate; RT, reverse transcriptase; TMD, transmembrane domain; RACE, rapid amplification of cDNA ends; PCR, polymerase chain reaction; HEPES, 4-(2-hydroxyethyl)-1-piperazineethanesulfonic acid.

TABLE 1

Primers used for PCR cloning of OCT1 cDNA

Restriction enzyme recognition sites incorporated into primer sequences are indicated by underlining.

Primer designation	Primer sequence
Primer 1	5'-ATGCCACCGTGGATGATGTCCTGG-3'
Primer 2	5'-AGTGCAGAACAGGTC-3'
5'-RACE-1	5'-AGCCGGGCGTGTCATACACCCA-3'
5'-RACE-2	5'-AGCGGCAGGTGGCTCCTGTTGG-3'
5'-RACE-3	5'-CACTGTATAGTTCAGCTCCTCC-3'
Anchor primer 1 ^a (5'-RACE)	5'-CUACUACUACUAGGCCACGTCGACTAGTACGGGIIIGGGIIIGGIIIG-3'
Anchor primer 2 ^a (5'-RACE)	5'-CUACUACUACUAGGCCACGTCGACTAGTAC-3'
3'-RACE-1	5'-TACTACTGGTGTGTGCCGAG-3'
3'-RACE-2	5'-ATCGCTCAAAAGAATGGGAAG-3'
Adapter primer ^a (3'-RACE)	5'-GGCCACGCGTCGACTAGTACTTTTTTTTTTTTTTTTTT-3'
Amplification primer ^a (3'-RACE)	5'-GGCCACGCGTCGACTAGTAC-3'
5'-End primer	5'- <u>GGAATTCC</u> CATCATGCCACCGTGGA-3'
	EcoRI site
3'-End primer	5'- <u>GCTCTAG</u> CAAAACATCTCTCTCA-3'
	XbaI site

^a These primers were provided with the 5'- and 3'-RACE system (GIBCO BRL).

Despite the critical role that hepatic transporters play in drug absorption and elimination and in detoxification, there have been few studies of hepatic transport of organic cations in humans (6, 10), and no study has elucidated the molecular structure or function of human polyspecific organic cation transporters in any tissue. In a recent study, notable species differences were observed in the rate of transport of the organic cation, vecuronium, in human hepatocytes in comparison to rat hepatocytes; the influx rate constant (k_{in}) of vecuronium in isolated rat hepatocytes was 10-fold greater than in human hepatocytes (6). Importantly, these interspecies differences in the rate of uptake of organic cations were also observed in the intact organ (11, 12).

In this study, we cloned and functionally characterized the first human organic cation transporter from liver (hOCT1). The sequence of hOCT1, its functional expression in *Xenopus laevis* oocytes and its tissue distribution are presented. Differences in the functional activity and tissue distribution of hOCT1 in comparison to rOCT1 were observed. Further studies of the function and regulation of hOCT1 will enhance our understanding of the mechanisms involved in organic cation transport in the human liver and the factors responsible for the observed interspecies differences.

Experimental Procedures

Isolation and subcloning of OCT1-like homologous PCR fragments from human liver cDNA. The cDNA template for PCR amplification was synthesized from human liver mRNA (Clontech, Palo Alto, CA) with the oligo(dT) primer using the SuperScript Preamplification System (GIBCO BRL, Gaithersburg, MD) according to the manufacturer's protocol. The primers 1 and 2 (Table 1) used in RT-PCR were designed from the conserved regions after alignment of several homologous genes, including rOCT1 (8) and OCT2, a rat kidney-specific organic cation transporter (designated rOCT2) (13). PCR was performed in a thermal cycler (Perkin-Elmer, Foster City, CA) set to the following parameters: 94° for 1 min, 48° for 2 min, 72° for 2 min, and 40 cycles followed by a final 15-min incubation at 72°. *Pfu* DNA polymerase (Stratagene, La Jolla, CA) was mixed with *Taq* DNA polymerase (v/v 1:15) in the reaction mixture to increase the fidelity of PCR.

The PCR products were electrophoresed through 1% agarose gel, and size-selected DNA fragments were extracted and ligated (subcloned) to the pGEM-T vector (Promega, Madison, WI) using T4 DNA ligase according to the T-A cloning method followed by transforma-

tion into DH5 α competent cells (GIBCO BRL). Plasmid DNA was isolated using the Wizard Miniprep DNA Purification System (Promega) and was analyzed by restriction enzyme analysis and/or sequencing.

DNA amplification of the cDNA 5' and 3' ends and the full-length cDNA. To obtain the remaining 5' portion of hOCT1 cDNA, a PCR-based method, 5' RACE was used. Three gene-specific antisense primers, designated 5'-RACE-1, 5'-RACE-2, and 5'-RACE-3 (see Table 1 for details of following procedure), were designed from the partial hOCT1 sequence (the sequenced PCR fragment). First-strand cDNA synthesis for 5'-RACE was primed with 5'-RACE-1 using the 5' RACE System for Rapid Amplification of cDNA Ends (GIBCO BRL) from human liver mRNA (Clontech). Homopolymeric tails were added to the 3' end of the cDNA, which was then amplified by PCR using the anchor primer 1 and nested 5'-RACE-2 primer. A nested PCR was performed with the anchor primer 2 and nested 5'-RACE-3 primer with a different annealing temperature (50°) to assess the specificity of the PCR product. The amplified products from the nested PCR were then subcloned as previously described.

3'-RACE protocol was used to obtain the remaining 3' portion of hOCT1 cDNA. Two gene-specific sense primers, designated 3'-RACE-1 and 3'-RACE-2 (see Table 1), were designed from the partial hOCT1 sequence (the sequenced PCR fragment). First-strand cDNA synthesis was initiated at the poly(A)⁺ tail of human liver mRNA (Clontech) using the adapter primer provided with the 3' RACE System for Rapid Amplification of cDNA Ends (GIBCO BRL) following the manufacturer's protocol. PCR was performed on this first-strand cDNA using 3'-RACE-1 primer and the nested amplification primer. The resulting amplified products from the nested PCR with 3'-RACE-2 primer and the amplification primer were then subcloned as described above.

The entire hOCT1 cDNA coding region was obtained by RT-PCR with the 5'-end primer and 3'-end primer (see Table 1), which were designed from the beginning and end regions of the open reading frame according to the following protocol: 94° for 1 min, 55° for 2 min, 72° for 2 min, and 35 cycles followed by a final 30-min incubation at 72°.

Sequence analysis. cDNA isolated from multiple RT-PCR were sequenced using universal and gene specific primers at the Biochemical Resource Center DNA Sequencing Facility (University of California, San Francisco) with an automated sequencer (model 373A; Applied Biosystems, Foster City, CA).

Multiple sequence alignments were produced using the Gap and Pileup programs in the Genetics Computer Group (Wisconsin Package, Version 8; Madison, WI) software package. The Motifs program in the Genetics Computer Group package was used to determine

potential protein kinase C phosphorylation sites and *N*-glycosylation sites. The TMDs of hOCT1 were predicted on the basis of hydropathy analysis using the Kyte-Doolittle algorithm (14) in the Genetics Computer Group Peplot program as well as the hydropathy analysis program in DNA Strider 1.2, a C program for DNA and protein analysis designed and written by Dr. C. Marck (Service de Biochimie et de Genetique Moleculaire, Gif-sur-Yvette, France).

Expression of hOCT1 in *X. laevis* oocytes and MPP⁺ and ¹⁴C-TEA transport measurements. Oocytes were harvested from *X. laevis* (Xenopus I, Ann Arbor, MI, and Nasco, Fort Atkinson, WI) and defolliculated with collagenase D (Boehringer-Mannheim Biochemicals, Indianapolis, IN) in a calcium-free OR II solution as previously described (15). Healthy stage V and VI oocytes were injected with 50 nl of diethylpyrocarbonate-treated water, mRNA, or 5–100 ng of capped cRNA transcribed *in vitro* with T7 RNA polymerase (mCAP RNA Capping Kit; Stratagene) from linearized plasmid DNA. The injected oocytes were maintained in modified Barth's solution at 18° before uptake experiments.

The uptake of ³H-MPP⁺ (79.9 Ci/mmol, DuPont-New England Nuclear, Boston, MA) or ¹⁴C-TEA (55 mCi/mmol, American Radiolabeled Chemicals, St. Louis, MO) in oocytes was measured as described previously (15). Briefly, groups of six to nine oocytes were incubated in a Na⁺-uptake buffer (100 mM NaCl, 2 mM KCl, 1 mM CaCl₂, 1 mM MgCl₂, 10 mM HEPES/Tris, pH 7.4) containing ³H-MPP⁺ (0.15 μM ³H-MPP⁺ and 0.7 μM unlabeled MPP⁺) or ¹⁴C-TEA (100 μM) at 25°. For inhibition studies, various unlabeled compounds (concentrations are specified in the figure legends) were included in the reaction mixture. For the Michaelis-Menten kinetics study, 0.15 μM ³H-MPP⁺ plus various amounts of unlabeled MPP⁺ were included in the reaction mixture. The K⁺-uptake buffer (2 mM NaCl, 100 mM KCl, 1 mM CaCl₂, 1 mM MgCl₂, 10 mM HEPES/Tris, pH 7.4) was used to test the potential-dependency. The resting membrane potentials of water and hOCT1 cRNA-injected oocytes incubated in the specified Na⁺ and K⁺ buffer were measured with the use of standard microelectrode techniques (16). In the pH-dependency studies, the K⁺ buffers were used at various pH levels (6.4, 7.4, and 8.4 in HEPES/Tris buffer). The radioactivity associated with each oocyte was assayed by liquid scintillation counting.

***In vitro* translation and sodium dodecyl sulfate-polyacrylamide gel electrophoresis gel analysis.** The TNT T7 Quick Coupled Transcription/Translation System (Promega) and L-³⁵S-methionine (1000 Ci/mmol, 10 mCi/ml, DuPont-New England Nuclear) were used for eukaryotic *in vitro* translation according to the manufacturer's protocol. Five microliters of translation products was denatured in 20 μl of Laemmli's sample buffer plus 5% (v/v) 2-mercaptoethanol at 75° for 10 min and loaded onto the 4–20% gradient gel (Tris-Glycine Ready Gels, BioRad, Hercules, CA). To increase the sensitivity of detection of ³⁵S-labeled proteins, the gel was soaked in Amplify (Amersham Life Science, Arlington Heights, IL) for 15–30 min after the fixing step. The gel was then dried and exposed to Hyperfilm-MP film (Amersham Life Science) overnight at –70° before development.

Northern analysis. A commercially available hybridization-ready blot containing poly(A)⁺ mRNA from different human tissues (Multiple Tissue Northern Blot, Clontech) was used in Northern blot analysis. The blot is from an agarose gel of 2 μg of poly(A)⁺ RNA from various human tissues. The blot was probed at 65° overnight with a full-length antisense cRNA probe. The probe was synthesized using BrightStar BiotinScript nonisotopic *in vitro* transcription kit (Ambion, Austin, TX) according to the manufacturer's protocol. After hybridization and stringent washings, the signals were detected using the BrightStar Nonisotopic Detection System (Ambion) followed by membrane exposure to Hyperfilm-ECL film (Amersham Life Science).

To check the quality and quantity of the poly(A)⁺ RNA of each tissue loaded onto the blot, the membrane was stripped and reprobed with a human β-actin cDNA probe. A prominent β-actin signal was observed in each lane of the blot (data not shown).

Data analysis. Uptake values are expressed as fmol/oocyte/hr or pmol/oocyte/hr and presented as mean ± standard error or as specified in the figure legends. A minimum of six to nine oocytes were used in each experiment. Statistical analysis was carried out by unpaired Student's *t* test, and a value of *p* < 0.05 was considered significant.

Materials. All chemicals were purchased from Sigma Chemical (St. Louis, MO) and Fisher Scientific (Pittsburgh, PA) or as indicated. Molecular biology enzymes, reagents, and kits and radiolabeled compounds were purchased from specific manufacturers as indicated. Primers were synthesized at Biochemical Resource Center (University of California, San Francisco) and GIBCO BRL.

Results

Molecular cloning of the full-length hOCT1 cDNA. An amplification product of ~1 kb in length was obtained when the PCR was performed with primers 1 and 2 and with human liver first-strand cDNA as template. DNA sequencing revealed that the PCR product was 1024 bp in length and 82% identical to the rOCT1 cDNA, suggesting that a partial cDNA encoding a human organic cation transporter had been obtained. To clone the full-length cDNA a PCR-based cloning strategy involving 5'- and 3'- RACE protocols was pursued (17, 18). The resulting 5'- (~280 bp) and 3'- (~900 bp) RACE products were derived from the partial human cDNA as indicated by sequence analysis, and the full-length cDNA was obtained by RT-PCR using primers flanking the 5' and 3' ends and human liver mRNA as the initial template. The resultant product (~1.7 kb) was subcloned into a TA-based vector; this human clone is designated hOCT1.

DNA sequencing and primary amino acid sequence. The nucleotide sequence and deduced primary amino acid sequence of the hOCT1 cDNA¹ are shown in Fig. 1, *top*. The cDNA is 1870 bp in length, including the poly(A)⁺ tail. The open reading frame is 1662 bp long and encodes a protein of 554 amino acids with a calculated molecular mass of 61 kDa. The predicted initiation codon is preceded by a Kozak consensus sequence (A/GXXAUG) (19). The putative 12 TMDs were predicted by a combination of Kyte-Doolittle hydropathy analysis (14) (Fig. 1, *bottom*), application of the positive-inside rule (20), and multiple sequence alignment analysis of hOCT1 and its related rat and mouse sequences (i.e., rOCT1, rOCT2, Lx1; Ref. 21). The protein sequence contains three potential *N*-linked glycosylation sites (N-X-T/S) at positions 71, 96, and 112. In addition, five potential protein kinase C phosphorylation sites were identified at residues 285, 291, 327, 340, and 524.

Functional expression and characterization in *X. laevis* oocytes. A significant increase in the cimetidine-inhibitable ³H-MPP⁺ uptake was observed in cRNA-injected oocytes (429 ± 36.8 fmol/oocyte/hr in the absence of 5 mM cimetidine versus 11.6 ± 0.933 fmol/oocyte/hr in the presence of 5 mM cimetidine, mean ± standard error, *p* < 0.01) at 3 days after injection (Fig. 2, *top*). [A 3-fold increase in the specific uptake (TEA inhibitable) of ¹⁴C-TEA (100 μM) over that in water-injected oocytes (3.83 ± 0.777 versus 1.29 ± 0.163 pmol/oocyte/hr, mean ± standard deviation) was observed, indicating that TEA is also a substrate (permeant) of the transporter.] ³H-MPP⁺ uptake in the cRNA-injected oo-

¹ The sequence reported here was submitted to GenBank with the accession number U77086.

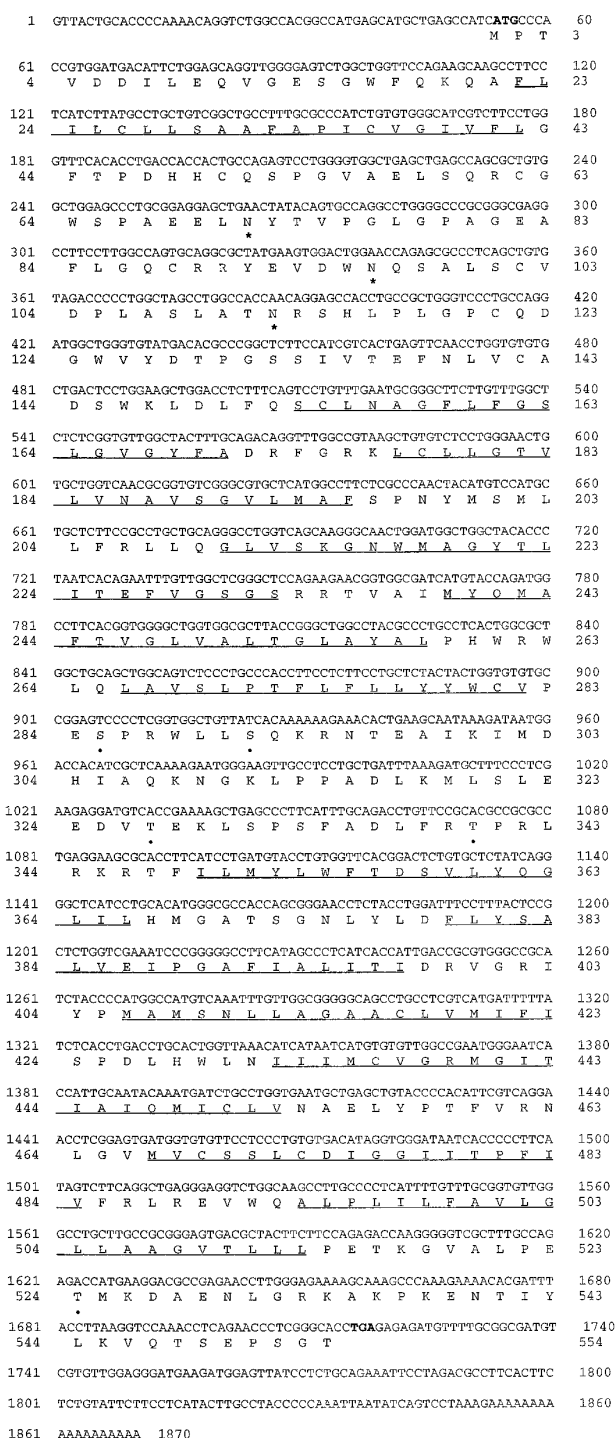


Fig. 1. *Top*, nucleotide and deduced amino acid sequences of hOCT1 cDNA. **Bold**, start (ATG) and stop (TGA) codons. Underlined, 12 putative TMDs; *, potential N-glycosylation sites of the type N-X-T/S; *points*, five potential protein kinase C phosphorylation sites. *Bottom*, Kyte-Doolittle hydropathy analysis of hOCT1 using a window of 11. Numbers 1–12, putative TMDs.

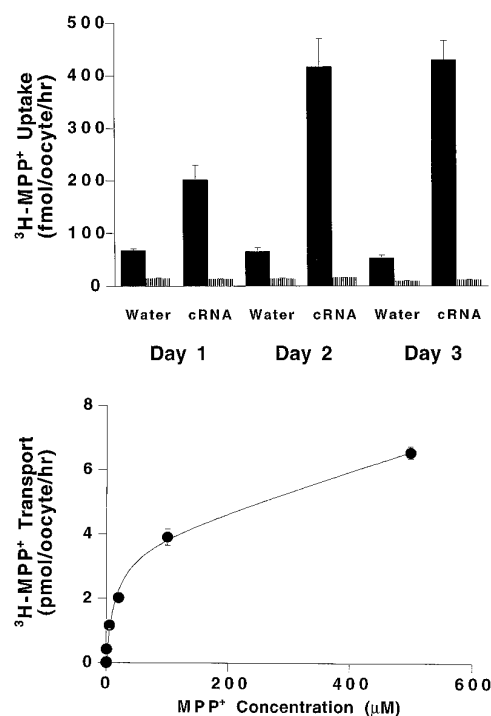


Fig. 2. Functional expression of hOCT1 in *X. laevis* oocytes. *Top*, ³H-MPP⁺ uptake in hOCT1 cRNA (25 ng)-injected oocytes compared with water (50 nl)-injected oocytes on day 1, 2, and 3 after injection. ³H-MPP⁺ (0.15 μM) uptake by oocytes was assayed for 90 min at 25°. *Columns*, mean ± standard error (seven to nine oocytes) of one representative experiment (■, uptake in the absence of 5 mM cimetidine; □, uptake in the presence of 5 mM cimetidine). *Bottom*, Kinetics of MPP⁺ transport in hOCT1 cRNA (25 ng)-injected oocytes. Data were fitted to the Michaelis-Menten equation. ($K_m = 14.6 \pm 4.39 \mu\text{M}$, $V_{\text{max}} = 3.69 \pm 0.409 \text{ pmol/oocyte/hr}$). *Points*, mean ± standard error (seven to nine oocytes) from one representative experiment.

cytes increased 8-fold over that in the water-injected oocytes ($53.0 \pm 6.40 \text{ fmol/oocyte/hr}$, mean ± standard error, $p < 0.01$) and ~3-fold over that in oocytes injected with poly(A)⁺ RNA (mRNA) from human liver (data not shown). The uptake of ³H-MPP⁺ in the oocytes was significantly higher than that in water-injected oocytes on day 1 and was further enhanced on days 2 and 3 after injection of the cRNA (Fig. 2, *top*). Subsequent uptake studies were carried out after ≥2 days of incubation after cRNA injection, as indicated in the figure legends.

The uptake of ³H-MPP⁺ was dependent on the injected dose of cRNA. In oocytes injected with 5, 10, 25, 50, and 100 ng of hOCT1 cRNA, the uptake of ³H-MPP⁺ was 107 ± 10.4 , 183 ± 14.7 , 376 ± 29.3 , 429 ± 36.8 , and $848 \pm 108 \text{ fmol/oocyte/hr}$ (mean ± standard error; eight or nine oocytes), respectively. However, the relative enhancement in ³H-MPP⁺ uptake varied depending on the batch of oocytes and cRNA integrity. ³H-MPP⁺ uptake was linear up to 120 min (data not shown); therefore, subsequent kinetic studies were carried out at 60–90 min.

The rate of MPP⁺ uptake (at 90 min) was saturable (Fig. 2, *bottom*). The data were found to fit best to a model incorporating a saturable process plus a simple diffusion term. The V_{max} and K_m values of MPP⁺ transport were $3.69 \pm 0.409 \text{ pmol/oocyte/hr}$ and $14.6 \pm 4.39 \mu\text{M}$, respectively.

Small organic cations significantly reduced the uptake of ³H-MPP⁺ (Fig. 3, *top left and right*, $p < 0.01$). The endoge-

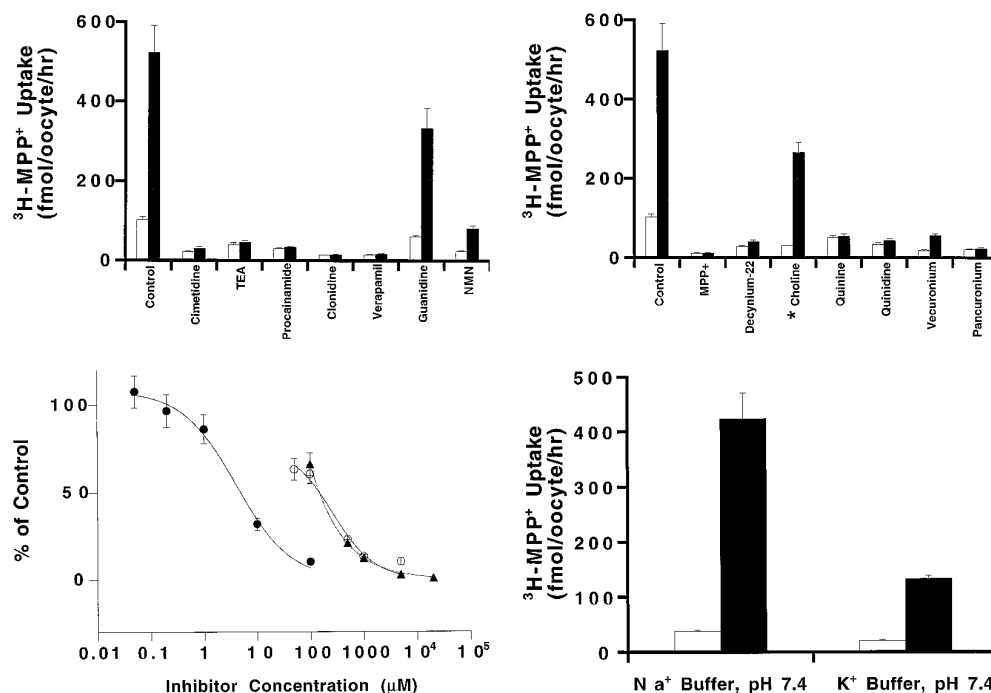


Fig. 3. Specificity of hOCT1 expressed in *X. laevis* oocytes. *Top left*, effect of various organic cations (5 mM) on $^3\text{H-MPP}^+$ uptake in oocytes injected with hOCT1 cRNA (■, 25 ng) and water (□). Uptake was assayed for 90 min on day 2 after injection; *columns*, mean \pm standard error (seven to nine oocytes) of one representative experiment; *NMN*, N^1 -methylthiothymine. *Top right*, effect of various organic cations (1 mM) on $^3\text{H-MPP}^+$ uptake in oocytes injected with hOCT1 cRNA (■, 25 ng) and water (□, 50 nl). Uptake was assayed for 90 min on day 2 after injection; *, control values for choline (1 mM) inhibition were 37.6 ± 2.65 fmol/oocyte/hr (water injected) and 424 ± 46.8 fmol/oocyte/hr (hOCT1 cRNA injected). Uptake was assayed for 60 min on day 4 after injection; *columns* mean \pm standard error (seven to nine oocytes) of one representative experiment. *Bottom left*, study of the effects of the organic cations decynium-22 (●), vecuronium (○), and TEA (▲) on $^3\text{H-MPP}^+$ uptake. $^3\text{H-MPP}^+$ uptake was assayed for 90 min on day 3 after injection in oocytes injected with hOCT1 cRNA (25 ng) or water (50 nl). The percentage of control was calculated after subtraction of MPP^+ uptake in water-injected oocytes. The data were fit to a logistic equation; *points*, mean \pm standard error (seven to nine oocytes) from one representative experiment. *Bottom right*, effect of membrane potential on $^3\text{H-MPP}^+$ uptake in oocytes injected with hOCT1 cRNA (■, 25 ng) and water (□, 50 nl). Uptake was assayed for 60 min on day 4 after injection; *points*, mean \pm standard error (seven to nine oocytes) from one representative experiment. Controls represent uptake in oocytes in the absence of inhibitors.

nous organic cation, guanidine (5 mM), was a weaker inhibitor ($p < 0.05$). In addition, bulkier organic cations, including the bivalent organic cations vecuronium and pancuronium, significantly inhibited $^3\text{H-MPP}^+$ uptake (Fig. 3, *top right*, $p < 0.01$). Further studies were performed to determine the IC_{50} values of decynium-22, vecuronium, and TEA (Fig. 3, *bottom left*). Decynium-22 ($\text{IC}_{50} = 4.70 \pm 1.28 \mu\text{M}$) was the most potent inhibitor of $^3\text{H-MPP}^+$, followed by vecuronium ($\text{IC}_{50} = 127 \pm 41.2 \mu\text{M}$) and TEA ($\text{IC}_{50} = 173 \pm 8.76 \mu\text{M}$). The bile acid taurocholate (5 mM and $100 \mu\text{M}$) and the nucleosides thymidine and inosine also significantly inhibited the uptake of $^3\text{H-MPP}^+$ ($p < 0.01$, Table 2). In contrast, D-glucose (5 mM) and the classic organic anion PAH (5 mM) showed no inhibition (Table 2).

The effects of pH and membrane potential on $^3\text{H-MPP}^+$ uptake in oocytes injected with hOCT1 cRNA were studied. When the pH of the medium was varied from 6.4 to 7.4, there was a significant change in $^3\text{H-MPP}^+$ uptake in cRNA-injected oocytes after subtraction of $^3\text{H-MPP}^+$ uptake in water-injected oocytes (pH 6.4, 100 ± 28.0 fmol/oocyte/hr; pH 7.4, 145 ± 51.3 fmol/oocyte/hr; pH 8.4, 120 ± 9.85 fmol/oocyte/hr, mean \pm standard deviation). The effect of membrane potential on $^3\text{H-MPP}^+$ uptake in cRNA-injected oocytes was determined. The membrane potential of oocytes in the Na^+ buffer was -32 ± 2 mV (mean \pm standard error, five oocytes), and the potential of oocytes was reduced to -13 ± 2 mV (mean \pm standard error, five oocytes) in the K^+ medium. $^3\text{H-MPP}^+$

uptake in cRNA-injected oocytes was significantly lower in K^+ medium compared with that in Na^+ medium ($p < 0.01$, Fig. 3, *bottom right*), suggesting that the transport of MPP^+ by hOCT1 is sensitive to membrane potential.

In vitro translation of hOCT1 mRNA. The translation product, as analyzed with the use of sodium dodecyl sulfate-polyacrylamide gel electrophoresis gel analysis, resulted in a single band with an apparent molecular size of ~ 47 kDa (not shown). This apparent molecular mass is smaller than that predicted value based on the deduced sequence (~ 61 kDa); however, anomalous migration (smaller-than-predicted sizes) for membrane proteins is not unusual.

Tissue distribution and expression of hOCT1 mRNA. The tissue distribution of hOCT1 mRNA transcripts was examined by Northern blot analysis (Fig. 4). A strong 2.0-kb hybridizing signal (the approximate molecular size of the mRNA transcript of hOCT1) as well as a weaker band at 4.3-kb (not shown) were detected only from liver mRNA (Fig. 4, *lane 5*). A weak 2.5-kb signal was detected in heart (*lane 1*), skeletal muscle (*lane 6*), and kidney (*lane 7*), and a very weak signal was detected in brain (*lane 2*) and placenta (*lane 3*). No signal was detected in lung (*lane 4*), pancreas (*lane 8*), or intestine (data not shown). These data suggest that hOCT1 mRNA transcript is expressed primarily in the human liver. (A full-length cDNA of hOCT1 was detected after RT-PCR from human kidney and intestine mRNA, suggesting that

TABLE 2

Uptake of $^3\text{H-MPP}^+$ in the presence of nonclassic organic cation transport inhibitors

The uptake of $^3\text{H-MPP}^+$ ($0.15 \mu\text{M}$) at 60 or 90 min in water- and hOCT1 cRNA-injected oocytes in the absence (control) and presence of various organic compounds was measured on day 3 or 4 after injection is described in Experimental Procedures. The data represent mean \pm standard error for seven to nine oocytes. All uptake values in cRNA-injected oocytes are significantly lower than control ($p < 0.05$) except those for PAH and D-glucose. Controls represent uptakes in the oocytes in the absence of inhibitors.

	Uptake of $^3\text{H-MPP}^+$ in water-injected oocytes	Uptake of $^3\text{H-MPP}^+$ in cRNA-injected oocytes
	<i>fmol/oocyte/hr</i>	
Day 3, 90 min		
Control	102 ± 7.79	523 ± 68.4
Taurocholate (5 mM)	78.4 ± 5.44	184 ± 4.78
PAH (5 mM)	349 ± 98.9	738 ± 86.1
D-glucose (5 mM)	133 ± 14.6	679 ± 46.2
Thymidine (5 mM)	142 ± 15.9	292 ± 9.00
Day 4, 60 min		
Control	37.6 ± 2.65	424 ± 46.8
Thymidine (1 mM)	28.3 ± 5.41	299 ± 23.7
Inosine (1 mM)	25.9 ± 3.26	178 ± 20.9
Taurocholate (100 μM)	44.6 ± 2.68	284 ± 28.1
Vecuronium (100 μM)	25.0 ± 1.22	232 ± 17.6

low copy numbers of the mRNA transcripts of hOCT1 may be present in these tissues.)

Homology of hOCT1 to other organic cation transporters. Computer-based homology search of GenBank, EMBL, and SwissProt 23 data bases indicated that the cloned hOCT1 cDNA has not been previously described. The hOCT1 cDNA clone shares the greatest homology with a group of organic cation transport proteins, including rOCT1, rOCT2 from rat kidney, and the recently cloned murine Lx1 gene (putative mouse OCT1 homologue). hOCT1 is homologous to rOCT1 (78% identity and 82% similarity in peptide sequence), Lx1 (78% identity and 82% similarity), and rOCT2 (64% identity and 73% similarity). In addition, hOCT1 is also homologous to a rat liver-specific transport protein, NLT (GenBank accession no. L27651, 31% identity and 52% similarity) and a mouse kidney-specific transporter protein (GenBank accession no. U52842, 32% identity and 40% similarity).

Peptide sequence alignment of rOCT1, Lx1, hOCT1, and

rOCT2 is shown in Fig. 5. Sequence alignment suggests that these proteins are related structurally and functionally. Notably, each is predicted to have 12 TMDs. In addition, rOCT1, rOCT2, and hOCT1 all transport TEA. However, the function of Lx1 has not been determined. Among the four proteins, rOCT1 and Lx1 are most homologous (95% identity). The alignment demonstrates that the sequence at the amino terminus and the first extracellular loop between TMDs 1 and 2 are most conserved among the three species. Three putative *N*-glycosylation sites for rOCT1, Lx1, and hOCT1 are conserved in the extracellular loop between TMDs 1 and 2, whereas only two are conserved in rOCT2. The *N*-glycosylation site in rOCT1 and Lx1 in the loop between TMDs 9 and 10 is lacking in both hOCT1 and rOCT2. Only one potential protein kinase C phosphorylation site is conserved in all four proteins (at the amino acid residue 285 of hOCT1 between TMDs 6 and 7), whereas two potential protein kinase C sites at 291 and 327 of hOCT1 are conserved in rOCT1, Lx1, and hOCT1. Other protein kinase C phosphorylation sites on hOCT1 (i.e., at positions 340 and 534) do not align. In addition, several conserved regions for the members of the transport proteins of family I, which include glucose transporters (22), were also observed. The first is a G(X)₃-D-R/K-X-G-R-R/K (or D-R/K-X-G-R) (Fig. 5, *motif 1*), which is conserved in the intracellular loop between TMDs 2 and 3 and TMDs 8 and 9. The second motif is EXXXXXXR (Fig. 5, *motif 2*), which is conserved between TMDs 4 and 5 and TMDs 10 and 11. The third set of conserved motifs includes the sequences of P-E-S-P-R-X-L and P-E-T-K (Fig. 5, *motif 3*) located after the predicted TMDs 6 and 12, respectively. These data indicate that hOCT1 along with rOCT1, Lx1, and rOCT2 belong to the transporter family I.

Discussion

Studies in which a variety of tissue preparations are used, including isolated hepatocytes, perfused liver, and isolated plasma membrane vesicles, as well as functional studies of the recently cloned polyspecific organic cation transporter (rOCT1) have greatly advanced our understanding of the mechanisms of organic cation transport in the rat liver (1–5,

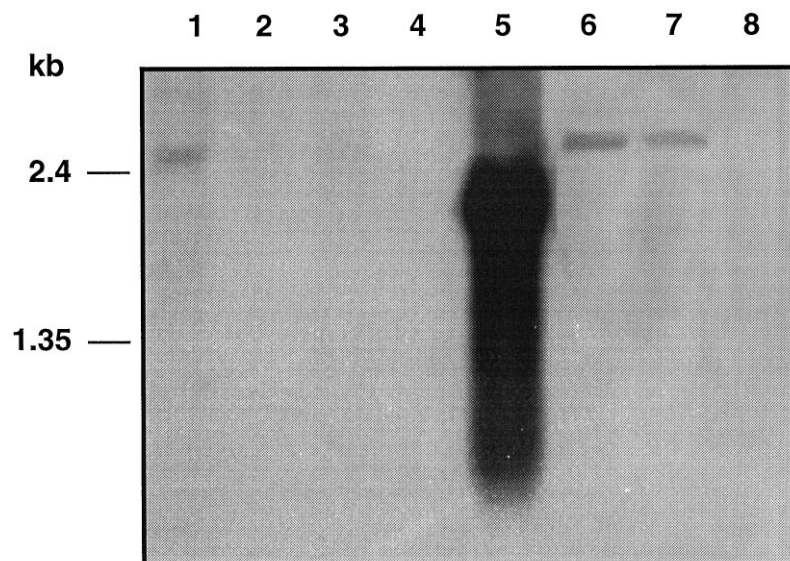


Fig. 4. Northern blot analysis of hOCT1 mRNA in various human tissues. A commercially available hybridization-ready blot composed of poly(A)⁺ mRNA from different human tissues (Multiple Tissue Northern Blot; Clontech) was hybridized with a full-length antisense cRNA probe representing the entire coding region of hOCT1. Lanes 1–8, mRNA samples (2 $\mu\text{g}/\text{lane}$) from heart, brain, placenta, lung, liver, skeletal muscle, kidney, and pancreas, respectively.

	1		50
rOCT1	MPTVDDVLEQ	VGEFGWFQKQ	AFLLLLCLISA SLAPIYVGIV FLGFTPDHHC
Lx1	MPTVDDVLEH	VGEFGWFQKQ	AFLLLLYLISA SLAPIYVGIV FLGFTPDHHC
hOCT1	MPTVDDILEQ	VGESGWFQKQ	AFLLLLCLISA AFAPICVGIV FLGFTPDHHC
rOCT2	MSTVDDILEH	IGEFHLFQKQ	TFFLLALLSG AFTPIYVGIV FLGFTPDHHC
	51		100
rOCT1	QNPVGAELSQ	RCGWSQAEEL	NYTVPGLGPS DEASFLSQCM RYEVDWQST
Lx1	RSPVGAELSQ	RCGWSQAEEL	NYTVPGLGPS GEASFLSQCM RYEVDWQST
hOCT1	QSPVGAELSQ	RCGWSQAEEL	NYTVPGLGPS GEA.FLGQCR RYEVDWQSA
rOCT2	WSPGAELSQ	RCGWSQAEEL	NYTVPGLGPS DEASFLSQCM RYEVDWQST
	101		150
rOCT1	LDCVDPLSSL	VANRSQPLPG	PCEHGWVYDT PGSSIVTEFN LVCGDAMKVD
Lx1	LDCVDPLSSL	AANRSHPLPS	PCEHGWVYDT PGSSIVTEFN LVCVDAMKVD
hOCT1	LSCVDPLASL	ATNRSQPLPG	PCQDGVYDT PGSSIVTEFN LVCADSWKLD
rOCT2	LDCVDPLSSL	AADRNLPLPG	PCDGHVYNT PGSSIVTEFN LVCADSWKLD
	151	motif 1	200
rOCT1	LFQSCVNLF	FLGSLVGYI	ADRFGRKLCL LVTTLVTSVS GVLTAVAPDY
Lx1	LFQSCVNLF	FLGSLVGYI	ADRFGRKLCL LVTTLVTSLS GVLTAVAPDY
hOCT1	LFQSCNLAF	LFGLSGVGYF	ADRFGRKLCL LGTVLVNAVS GVLMASFENY
rOCT2	LFQSVNVGF	FIGAMISGYL	ADRFGRKLCL LVTTILINIS GALMAISFNY
	201	motif 2	250
rOCT1	TSMLLFRLLQ	GMVSKGSWVS	GYTLITEFVG SGYRRTTAIL YQMAFTVGLV
Lx1	TSMLLFRLLQ	GMVSKGSWVS	GYTLITEFVG SGYRRTTAIL YQMAFTVGLV
hOCT1	MSMLLFRLLQ	GLVSKGNWMA	GYTLITEFVG SGSRRTVAIM YQMAFTVGLV
rOCT2	AMMLVFRFLQ	GLVSKAGWLI	GYILITEFVG LGYRKMVGIC YQIAFTVGLL
	251	motif 3	300
rOCT1	GLAGVAYAI	DWRWLQAVS	LPTFLFLLY WFPVPEPRWL LQKRTTQAV
Lx1	GLAGVAYAI	DWRWLQAVS	LPTFLFLLY WFPVPEPRWL LQKRTTQAV
hOCT1	ALTGLAYALP	HWRWLQAVS	LPTFLFLLY WCVPEPRWL LQKRTTQAI
rOCT2	ILAGVAYVIP	NWRWLQAVT	LPNFCFLLYF WCIPEPRWL LQKRTTQAI
	301		350
rOCT1	RIMEQIAQKN	GKVPADLKM	LCLEEDAEEK RSPSFADLFR TPNLRKHFTVI
Lx1	RIMEQIAQKN	RKVPPADLKM	MCLEEDAEEK RSPSFADLFR TPRLRKHTVI
hOCT1	KIMDHIAQKN	GKLPADLKM	LSLEEDVTEK LSPSFADLFR TPRLRKHTVI
rOCT2	KIKKHIAKKN	GKSVFVSLQN	LTPBEDAGKK LKPSILDLVR TPQIRKHTLI
	351	motif 1	400
rOCT1	LMYLVFSCAV	LYQGLIMHVG	ATGANLYLDF FYSSLVEFPA AFIIILVTIDR
Lx1	LMYLVFSCAV	LYQGLIMHVG	ATGANLYLDF FYSSLVEFPA AFIIILVTIDR
hOCT1	LMYLVFSDSV	LYQGLILHMG	ATSGNLYLDF LYSALVEIPG AFIALITIDR
rOCT2	LMYNWFTSSV	LYQGLIMHMG	LAGDNLYLDF FYSALVEFPA AFIIILVTIDR
	401		450
rOCT1	IGRLTYPIAAS	NLVGTGAACLL	MIFIPHELHW LNVTACLGR MGATIVLQMV
Lx1	IGRLTYPIAAS	NLVGTGAACLL	MIFIPHELHW LNVTACLGR MGATIVLQMV
hOCT1	VGRITYPIAAS	NLLAGAACL	MIFISPDLHW LNIIMCVGR MGITIAIQMI
rOCT2	VGRITYPIAAS	NMVAGAACL	SVFIPDDLQW LKRTIACLGR MGITMAYEMV
	451	motif 2	500
rOCT1	CLVNAELYPT	FIRNLGMVVC	SALCDLGGIF TPFMVFLRME VQQAFLPLIF
Lx1	CLVNAELYPT	FIRNLGMVVC	SALCDLGGIF TPFMVFLRME VQQAFLPLIF
hOCT1	CLVNAELYPT	FVRNLGMVVC	SSLCDIGGII TPFIVFLRME VQQAFLPLIF
rOCT2	CLVNAELYPT	YIRNLGVLC	SSMCDIGGII TCFVLVRLTD IVMPEPLVVF
	501	motif 3	550
rOCT1	GVGLGTAGAM	TLLLPETKGV	ALPETIEEAE NLGRRKSKAK ENTIIYLQVQT
Lx1	GVGLGTAGAV	TLLLPETKGV	ALPETIEEAE NLGRRKSKAK ENTIIYLQVQT
hOCT1	AVGLGLAAGV	TLLLPETKGV	ALPETIEEAE NLG.RKAKPK ENTIIYLQVQT
rOCT2	AVVGLVAGAL	TLLLPETKGV	ALPETIEDAE NMQRPRKKR KENLPPSQAS
	551		593
rOCT1	GKSSST		
Lx1	GKSPHT		
hOCT1	SEPSGT		
rOCT2	RP@AKLRKRG	IIAAGADFAL	SEARDGASLS PPPKPTQTNL TYP

Fig. 5. Alignment of amino acid sequence of rOCT1, Lx1, hOCT1, and rOCT2 using Pileup program. *Single letters*, amino acids; *periods*, gaps introduced to generate this alignment; *bold*, putative N-glycosylation sites; *outlined letters*, potential protein kinase C phosphorylation sites; *open rectangles*, amino acid motif characteristics for a number of family I transmembrane transporters found within sequences. *Motif 1* [G-(X)3-D-R/K-X-G-R-R/K or D-R/K-X-G-R] between TMDs 2 and 3 and TMDs 8 and 9, predicted to form β -loops. *Motif 2* (E-X-X-X-X-X-R between TMDs 4 and 5 and TMDs 10 and 11) and *Motif 3* (P-E-S-P-R-X-L and P-E-T-K after TMD 6 and TMD 12, respectively), specific for family I transporter.

7–9, 23). In contrast, there have been few studies in which the mechanisms of organic cation transport in the human liver were examined (6, 10), and no study has elucidated the molecular structure or function of polyspecific organic cation

transporters in human liver or other human tissue. Limited data suggest that there are large differences in the rate of uptake of organic cations in human and rat hepatocytes (6).

In this study, we used information from the published sequences of recently cloned polyspecific organic cation transporters from rat to clone hOCT1, which is 78% identical and 82% similar to both rOCT1 and Lx1 (Figs. 1 and 5). We observed that the small organic cation MPP⁺ was a permeant of hOCT1 (Fig. 2). The uptake of MPP⁺ was inhibited by small organic cations (Fig. 3, *top left and right*) as well as by bulky organic cations pancuronium and vecuronium. These data are consistent with functional studies of rOCT1 (9, 23) and with the characteristics of the type I transporter in the rat hepatocyte that accepts small monovalent organic cations but can be inhibited by larger type II molecules (5). These characteristics are also consistent with the multispecific non-charge-selective transporter that accepts both large and small organic cations as well as other compounds (7). Similar to the type I carrier and rOCT1, hOCT1 seems to be sensitive to membrane potential (Fig. 3, *bottom right*).

In contrast to previous studies documenting no effect of the organic anion taurocholate on the transport of organic cations by the type I carrier in rat liver (24, 25), taurocholate (100 μ M and 5 mM) significantly inhibited the uptake of MPP⁺ in oocytes expressing hOCT1 (Table 2). These data suggest that hOCT1 is not charge selective with respect to bulky organic compounds and are consistent with the characteristics of the multispecific non-charge-selective transporter (7). It is possible that the interaction of taurocholate with hOCT1 represents a species difference in the selectivity of the two transporters. However, because no data are available, it is unclear whether taurocholate also interacts with rOCT1.

To determine whether there are interspecies differences in the kinetics of interaction of organic cations with the human (hOCT1) and rat (rOCT1) transporters, we determined the K_m value (or K_i , assuming a competitive inhibition model) of several organic cations. The K_m value (14.6 μ M) of the small organic cation MPP⁺ for hOCT1 is similar to that reported previously for rOCT1 (13 μ M) (8). In contrast, the K_i value of TEA (163 μ M) in inhibiting MPP⁺ uptake in oocytes expressing hOCT1 is somewhat higher than the reported K_m value of TEA (95 μ M) uptake in oocytes expressing rOCT1. Notably, the K_i value (4.4 μ M) of the large organic cation decynium-22 in oocytes expressing hOCT1 is considerably higher than that observed previously (0.36 μ M) for rOCT1 (8). These data indicate that there are important interspecies differences in the affinity of organic cations for hepatic organic cation transporters. A detailed characterization of the structure-activity relationships of each of the transporters (i.e., hOCT1 and rOCT1) is important to understand the interspecies differences in the uptake of organic cations in the human and rat liver.

Previous data suggest that the organic cation vecuronium is transported at a considerably slower rate in human hepatocytes in comparison to rat hepatocytes (6). Notably, the functional rate of uptake of vecuronium in cultured human hepatocytes is one-10th that in rat hepatocytes, suggesting that the relevant transporter or transporters in the human hepatocyte have a lower activity than that in the rat. The data suggest that the functional activity of organic cation transporter or transporters in the human liver involved in

the transport of vecuronium may be lower than that in the rat liver.

A lower functional activity may be a result of a higher K_m or lower V_{max} value. The K_i value of vecuronium obtained in this study (120 μ M) is \sim 10-fold the K_m value of vecuronium in the intact rat hepatocyte (26) and \geq 3-fold the IC_{50} value of vecuronium in interaction with the rat type I organic cation transporter (7). Thus, the lower affinity of vecuronium for hOCT1 may explain, in part, its lower rate of transport in the human hepatocyte. However, a compound may inhibit transport without being translocated, and further studies are needed to determine whether vecuronium is an actual permeant of hOCT1.

In this study, the V_{max} value of MPP⁺ transport in oocytes injected with the cRNA of hOCT1 (25 ng) was 3.7 pmol/oocyte/hr (Fig. 2, bottom), whereas in a previous study of oocytes injected with the cRNA of rOCT1 (8 ng) (8), the V_{max} value was 97 pmol/oocyte/hr. In addition, the uptake of TEA (100 μ M) was markedly lower in oocytes expressing hOCT1 than in oocytes expressing rOCT1 ($<$ 3-fold enhanced for hOCT1 in comparison to \sim 100-fold enhanced for rOCT1) (8). (Because of the low uptake values of TEA, we were unable to obtain a value for V_{max} .) Collectively, the results suggest that the V_{max} value of small organic cations is substantially lower in oocytes expressing hOCT1 than in oocytes expressing rOCT1. These data are consistent with previous studies suggesting that transporters in human hepatocytes have a much lower functional activity compared with those in rat hepatocytes (6). However, V_{max} values may differ between laboratories because of differences in experimental conditions and batches of oocytes. The availability of the cloned transporters (hOCT1 and rOCT1) will allow the development of antibodies to investigate, in detail, the mechanisms (e.g., differences in turnover rate or differences in the number of functional transporters) responsible for the observed interspecies differences in the activity of the transporters.

Organic cations are taken up by epithelial cells of the liver, kidney, and intestine (27–31). In agreement with its functional role in the various epithelia, the mRNA transcripts of rOCT1 and its mouse homologue, Lx1, were found in the kidney, liver, intestine, and colon (8, 21). In striking contrast, the mRNA transcript of hOCT1 is predominant in human liver (Fig. 4), with minor bands detected at 2.5 kb (a putative hOCT1 homologue) in heart, kidney, and skeletal muscle. It will be important to determine the transcription (or other) factors that are involved in the tissue-specific distribution of hOCT1 compared with rat and mouse homologous proteins. In addition, these data have important implications for the understanding of the differences in the mechanisms of organic cation transport in the various epithelia. For example, it is well known that the characteristics of organic cation transport differ between liver and kidney (29); in fact, certain organic cations are eliminated exclusively in the liver and not the kidney, and vice versa. Because hOCT1 is liver specific, our data suggest that other transporters are responsible for the secretion of organic cations in nonhepatic epithelia. With the availability of the cloned transporters, we can begin to understand the organ-specific elimination of drugs.

In conclusion, we cloned hOCT1, a polyspecific organic cation transporter from human liver. This transporter represents the first polyspecific organic cation transporter cloned from human tissue. The transporter is similar in sequence to

rOCT1, but notable differences in the kinetics of interaction of some organic cations were observed. Moreover, in contrast to rOCT1 and Lx1, Northern blot analysis suggests that the mRNA transcript of hOCT1 is preferentially expressed in human liver. The cloning of hOCT1 provides the opportunity to define the pharmacological profiles of this gene product and to determine its functional role in the disposition of many clinically used drugs and other xenobiotics.

References

- Groothuis, G. M., and D. K. Meijer. Drug traffic in the hepatobiliary system. *J. Hepatol.* **24** (Suppl. 1):3–28 (1996).
- McKinney, T. D., and M. A. Hosford. Organic cation transport by rat hepatocyte basolateral membrane vesicles. *Am. J. Physiol.* **263**:G939–G946 (1992).
- Meijer, D. K., W. E. Mol, M. Muller, and G. Kurz. Carrier-mediated transport in the hepatic distribution and elimination of drugs, with special reference to the category of organic cations. *J. Pharmacokinet. Biopharm.* **18**:35–70 (1990).
- Moseley, R. H., S. M. Jarose, and P. Permod. Organic cation transport by rat liver plasma membrane vesicles: studies with tetraethylammonium. *Am. J. Physiol.* **263**:G775–G785 (1992).
- Oude Elferink, R. P., D. K. Meijer, F. Kuipers, P. L. Jansen, A. K. Groen, and G. M. Groothuis. Hepatobiliary secretion of organic compounds: molecular mechanisms of membrane transport. *Biochim. Biophys. Acta* **1241**: 215–268 (1995).
- Sandker, G. W., B. Weert, P. Olinga, H. Wolters, M. J. Slooff, D. K. Meijer, and G. M. Groothuis. Characterization of transport in isolated human hepatocytes: a study with the bile acid taurocholic acid, the uncharged ouabain and the organic cations vecuronium and rocuronium. *Biochem. Pharmacol.* **47**:2193–2200 (1994).
- Steen, H., M. Merema, and D. K. Meijer. A multispecific uptake system for taurocholate, cardiac glycosides and cationic drugs in the liver. *Biochem. Pharmacol.* **44**:2323–2331 (1992).
- Grundemann, D., V. Gorboulev, S. Gambaryan, M. Veyhl, and H. Koepsell. Drug excretion mediated by a new prototype of polyspecific transporter. *Nature (Lond.)* **372**:549–552 (1994).
- Busch, A. E., S. Quester, J. C. Ulzheimer, S. Waldegger, V. Gorboulev, P. Arndt, F. Lang, and H. Koepsell. Electrogenic properties and substrate specificity of the polyspecific rat cation transporter rOCT1. *J. Biol. Chem.* **271**:32599–32604 (1996).
- Steen, H., and D. Meijer. Organic cations. *Prog. Pharmacol. Clin. Pharmacol.* **8**:239–272 (1991).
- Sohn, Y. J., A. F. Bencini, A. H. Scaf, U. W. Kersten, and S. Agoston. Comparative pharmacokinetics and dynamics of vecuronium and pancuronium in anesthetized patients. *Anesth. Analg.* **65**:233–239 (1986).
- Waser, P. G., H. Wiederkehr, A. C. Sin-Ren, and E. Kaiser-Schonenberger. Distribution and kinetics of ¹⁴C-vecuronium in rats and mice. *Br. J. Anaesth.* **59**:1044–1051 (1987).
- Okuda, M., H. Saito, Y. Urakami, M. Takano, and K. Inui. cDNA cloning and functional expression of a novel rat kidney organic cation transporter, OCT2. *Biochem. Biophys. Res. Commun.* **224**:500–507 (1996).
- Kyte, J., and R. F. Doolittle. A simple method for displaying the hydrophobic character of a protein. *J. Mol. Biol.* **157**:105–132 (1982).
- Giacomini, K. M., D. Markovich, A. Werner, J. Biber, X. Wu, and H. Murer. Expression of a renal Na(+)-nucleoside cotransport system (N2) in *Xenopus laevis* oocytes. *Pflueg. Arch. Eur. J. Physiol.* **427**:381–383 (1994).
- Quick, M. W., and H. A. Lester. Methods for expression of excitability proteins in *Xenopus* oocytes, in *Methods in Neuroscience* (P. M. Conn, ed.). Academic Press, San Diego, 261–279 (1994).
- Frohman, M. A., M. K. Dush, and G. R. Martin. Rapid production of full-length cDNAs from rare transcripts: amplification using a single gene-specific oligonucleotide primer. *Proc Natl Acad Sci USA* **85**:8998–9002 (1988).
- Schaefer, B. C. Revolutions in rapid amplification of cDNA ends: new strategies for polymerase chain reaction cloning of full-length cDNA ends. *Anal. Biochem.* **227**:255–273 (1995).
- Kozak, M. The scanning model for translation: an update. *J. Cell Biol.* **108**:229–241 (1989).
- von Heijne, G. Membrane protein structure prediction: hydrophobicity analysis and the positive-inside rule. *J. Mol. Biol.* **225**:487–494 (1992).
- Schweifer, N., and D. P. Barlow. The Lx1 gene maps to mouse chromosome 17, and codes for a protein that is homologous to glucose and polyspecific transmembrane transporters. *Mamm. Genome* **7**:735–740 (1996).
- Griffith, J. K., M. E. Baker, D. A. Rouch, M. G. Page, R. A. Skurray, I. T. Paulsen, K. F. Chater, S. A. Baldwin, and P. J. Henderson. Membrane transport proteins: implications of sequence comparisons. *Curr. Opin. Cell Biol.* **4**:684–695 (1992).
- Martel, F., T. Vetter, H. Russ, D. Grundemann, I. Azevedo, H. Koepsell, and E. Schomig. Transport of small organic cations in the rat liver: the role of the organic cation transporter OCT1. *Naunyn-Schmiedeberg's Arch. Pharmacol.* **354**:320–326 (1996).

24. Vonk, R. J., E. Scholtens, G. T. Keulemans, and D. K. Meijer. Cholerisis and hepatic transport mechanisms. IV. Influence of bile salt cholerisis on the hepatic transport of the organic cations, D-tubocurarine and N4-acetyl procainamide ethobromide. *Naunyn-Schmiedeberg's Arch. Pharmacol.* **302**:1–9 (1978).
25. Vonk, R. J., P. A. Jekel, K. F. Meijer, and M. J. Hardonk. Transport of drugs in isolated hepatocytes: the influence of bile salts. *Biochem. Pharmacol.* **27**:397–405 (1978).
26. Mol, W. E., G. N. Fokkema, B. Weert, and D. K. Meijer. Mechanisms for the hepatic uptake of organic cations: studies with the muscle relaxant vecuronium in isolated rat hepatocytes. *J. Pharmacol. Exp. Ther.* **244**:268–275 (1988).
27. Gramatte, T., R. Oertel, B. Terhaag, and W. Kirch. Direct demonstration of small intestinal secretion and site-dependent absorption of the beta-blocker talinolol in humans. *Clin. Pharmacol. Ther.* **59**:541–549 (1996).
28. Ott, R. J., A. C. Hui, G. Yuan, and K. M. Giacomini. Organic cation transport in human renal brush-border membrane vesicles. *Am. J. Physiol.* **261**:F443–F451 (1991).
29. Pritchard, J. B., and D. S. Miller. Mechanisms mediating renal secretion of organic anions and cations. *Physiol. Rev.* **73**:765–796 (1993).
30. Wright, S. H., and T. M. Wunz. Transport of tetraethylammonium by rabbit renal brush-border and basolateral membrane vesicles. *Am. J. Physiol.* **253**:F1040–F1050 (1987).
31. Turnheim, K., and F. Lauterbach. Secretion of monoquaternary ammonium compounds by guinea pig small intestine in vivo. *Naunyn-Schmiedeberg's Arch. Pharmacol.* **299**:201–205 (1977).

Send reprint requests to: Kathleen M. Giacomini, Ph.D., University of California, San Francisco, School of Pharmacy, Department of Biopharmaceutical Sciences, San Francisco, CA 94143. E-mail: kmg@itsa.ucsf.edu
